

# Effects of cubic BN addition and phase transformation on hardness of Al<sub>2</sub>O<sub>3</sub>–cubic BN composites

Mikinori Hotta\*, Takashi Goto

*Institute for Materials Research, Tohoku University, 2-1-1, Katahira, Aoba-ku, Sendai 980-8577, Japan*

Received 24 February 2010; received in revised form 1 July 2010; accepted 22 September 2010

Available online 24 February 2011

## Abstract

The Vickers hardness of dense Al<sub>2</sub>O<sub>3</sub>–cubic BN (cBN) composites prepared by spark plasma sintering under a moderate pressure of 100 MPa at 1200–1600 °C was investigated at indentation loads of 0.098–19.6 N. The BN grains in the Al<sub>2</sub>O<sub>3</sub>–BN composite prepared at 1300 °C showed no transformation from the cBN to hBN phase, and the hardness was 59 GPa at 0.098 N. The hardness of the Al<sub>2</sub>O<sub>3</sub> matrix in the Al<sub>2</sub>O<sub>3</sub>–BN composites containing 10–30 vol% cBN prepared at 1300–1400 °C was around 25 GPa at 0.098 N, which was higher than monolithic Al<sub>2</sub>O<sub>3</sub> bodies prepared at the same temperatures. The hardness of the Al<sub>2</sub>O<sub>3</sub> matrix in the Al<sub>2</sub>O<sub>3</sub>–BN composites decreased with increasing sintering temperature. The increase in the hardness of the Al<sub>2</sub>O<sub>3</sub> matrix may be due to the decrease in the size of Al<sub>2</sub>O<sub>3</sub> grains in the Al<sub>2</sub>O<sub>3</sub>–BN composites owing to the addition of cBN particles and the decrease in sintering temperature. The Meyer exponents of the monolithic Al<sub>2</sub>O<sub>3</sub> bodies and Al<sub>2</sub>O<sub>3</sub>–BN composites were 1.90–1.94 independent of cBN content.

© 2011 Elsevier Ltd and Techna Group S.r.l. All rights reserved.

**Keywords:** A. Sintering; B. Composites; C. Hardness; D. Nitrides

## 1. Introduction

Cubic boron nitride (cBN) and several ceramics such as Al<sub>2</sub>O<sub>3</sub>, TiN and Si<sub>3</sub>N<sub>4</sub> are widely used as cutting tools for high-speed machining for hard materials. cBN and Al<sub>2</sub>O<sub>3</sub> have high hardness, whereas their fracture toughness is lower than that of cutting tool material of WC–Co composite. Owing to the typical toughening mechanism of crack deflection, the fracture toughness can be improved by making composite materials. Next to diamond, cBN has the highest hardness, whereas it is hardly densified by conventional sintering mainly due to its strong covalent nature and phase transformation to low-hardness hexagonal BN (h-BN). In general, cBN sintered bodies are produced at an ultra-high pressure of more than 5 GPa and a high temperature of 1000–1400 °C with various additives such as Al, Ti, TiN and TiC [1–4]. Such an extreme high-pressure condition suppresses the phase transformation

from cBN to hBN at high temperature. Therefore, it is difficult to prepare fully dense cBN [5–7] and cBN-based composites [8,9] under a moderate pressure of less than 100 MPa.

We have reported the preparation of Al<sub>2</sub>O<sub>3</sub>–cBN [10], βSiAlON–cBN [11], TiN–cBN [12] and mullite–cBN [13] composites containing 10–20 vol% cBN at a moderate pressure of 100 MPa by spark plasma sintering (SPS). The densification of these composites was achieved without the phase transformation from cBN to hBN. The hardness is a primal issue for the application to cutting tools.

In the present study, the Vickers micro-hardness of BN grains and Al<sub>2</sub>O<sub>3</sub> matrix in Al<sub>2</sub>O<sub>3</sub>–BN composites prepared from Al<sub>2</sub>O<sub>3</sub> and cBN powders by SPS were measured at different indentation loads, and the effects of cBN addition, phase transformation and microstructure on the hardness of the Al<sub>2</sub>O<sub>3</sub>–BN composites were studied.

## 2. Experimental procedure

Al<sub>2</sub>O<sub>3</sub> (TM-DAR, Taimei Chemicals Co., Ltd., Nagano, Japan, average particle size: 0.2 μm) and cBN (SBN-F, Showa Denko K.K., Tokyo, Japan, average particle size: 2.8 μm) powders were used in the present study. The mixed powder was

\* Corresponding author. Present address: Advanced Manufacturing Research Institute, National Institute of Advanced Industrial Science and Technology (AIST), 2266-98 Shimo-Shidami, Moriyama-ku, Nagoya 463-8560, Japan. Tel.: +81 52 736 7120; fax: +81 52 736 7405.

E-mail address: [mikinori-hotta@aist.go.jp](mailto:mikinori-hotta@aist.go.jp) (M. Hotta).

sintered at temperatures ranging from 1200 to 1600 °C for 600 s in a vacuum under a uniaxial pressure of 100 MPa at a heating rate of 1.7 °C/s using an SPS apparatus (SPS-210LX, SPS Syntex Inc., Kanagawa, Japan). The detailed procedure of the SPS process has been reported elsewhere [10]. The relative densities of the Al<sub>2</sub>O<sub>3</sub> bodies reached more than 99% [10]. The relative densities of the Al<sub>2</sub>O<sub>3</sub>–BN composites were the same value as approximately 98% in all the composites [10]. The surface of specimens was ground with a diamond wheel and then finally polished with 1-μm diamond slurry. The Vickers hardness was measured at a load between 0.098 and 19.6 N using a micro-hardness tester (HM-221, Mitutoyo Corp., Kanagawa, Japan). The load was applied for 30 s. The hardness was calculated by the following formula:

$$H_V = 1854 \frac{P}{d^2}, \quad (1)$$

where  $P$  is the applied load and  $d$  is the average value of two diagonal lengths for Vickers indentation. The relationship between  $P$  and  $d$  can be expressed by the Meyer equation:

$$P = ad^n, \quad (2)$$

where  $a$  and Meyer exponent  $n$  are constant depending on the materials [14]. The relationship between  $H_V$  and  $P$  can be obtained from Eqs. (1) and (2) as follows:

$$H_V = 1854ad^{n-2}. \quad (3)$$

Hence, the hardness is independent of the indentation size at  $n = 2$ . The average value of 20 measurements at each specimen was used for the evaluation of the Vickers hardness. The indented surface was observed by scanning electron microscopy (SEM; S-3100H, Hitachi Ltd., Tokyo, Japan). The average size of Al<sub>2</sub>O<sub>3</sub> grains in the specimens was determined from linear intercept length of 100 grains in the SEM images.

### 3. Results and discussion

#### 3.1. Hardness of Al<sub>2</sub>O<sub>3</sub> matrix and BN grains in the composites

Fig. 1 shows the Vickers hardness of the Al<sub>2</sub>O<sub>3</sub> matrix and BN grains in the Al<sub>2</sub>O<sub>3</sub>–BN composites originally containing 10–30 vol% cBN and of monolithic Al<sub>2</sub>O<sub>3</sub> bodies prepared at 1200–1600 °C at a load of 0.098 N. The hardness of monolithic Al<sub>2</sub>O<sub>3</sub> bodies prepared at 1200–1400 °C was 19–20 GPa, and slightly decreased with increasing sintering temperature. When the sintering temperature was elevated from 1400 to 1600 °C, the hardness of the monolithic Al<sub>2</sub>O<sub>3</sub> bodies significantly increased from 19 to 23 GPa. In contrast, it has been reported that the hardness of monolithic Al<sub>2</sub>O<sub>3</sub> bodies at a load of 0.98 N decreased with increasing sintering temperature [10].

In the Al<sub>2</sub>O<sub>3</sub>–BN composite originally containing 20 vol% cBN, the hardness of BN grains reached 59 GPa without the phase transformation of cBN to hBN at 1300 °C. The cBN grains started to transform into the hBN phase at 1400 °C, and the Vickers hardness of the BN grains slightly decreased to 57 GPa. It was not possible to measure the hardness of BN

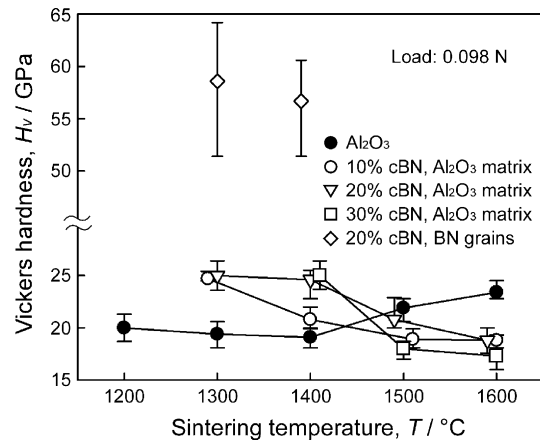


Fig. 1. Vickers hardness of Al<sub>2</sub>O<sub>3</sub> matrix and BN grains in Al<sub>2</sub>O<sub>3</sub>–BN composites originally containing 10–30 vol% cBN and Al<sub>2</sub>O<sub>3</sub> bodies sintered at 1200–1600 °C for 600 s at applied indentation load of 0.098 N.

grains prepared at 1500–1600 °C because of a porous microstructure resulting from the phase transformation into hBN [10].

The Al<sub>2</sub>O<sub>3</sub> matrix in the Al<sub>2</sub>O<sub>3</sub>–BN composites containing 10–20 vol% cBN prepared at 1300 °C without the phase transformation into hBN had the highest hardness of 25 GPa. With increasing sintering temperature, the Vickers hardness of the Al<sub>2</sub>O<sub>3</sub> matrix in the Al<sub>2</sub>O<sub>3</sub>–BN composites decreased. This was opposite to the trend of the monolithic Al<sub>2</sub>O<sub>3</sub> bodies, as shown in Fig. 1.

#### 3.2. Effect of size of Al<sub>2</sub>O<sub>3</sub> grains on hardness of Al<sub>2</sub>O<sub>3</sub> matrix

Fig. 2 demonstrates the effect of average size of Al<sub>2</sub>O<sub>3</sub> grains in the monolithic Al<sub>2</sub>O<sub>3</sub> bodies and the Al<sub>2</sub>O<sub>3</sub>–BN composites on Vickers hardness of the Al<sub>2</sub>O<sub>3</sub> matrix at a load of 0.098 N. The hardness of the monolithic Al<sub>2</sub>O<sub>3</sub> bodies decreased with increasing grain size from 0.6 to 4.5 μm obeying the Hall–Petch relationship [15,16], whereas the hardness significantly

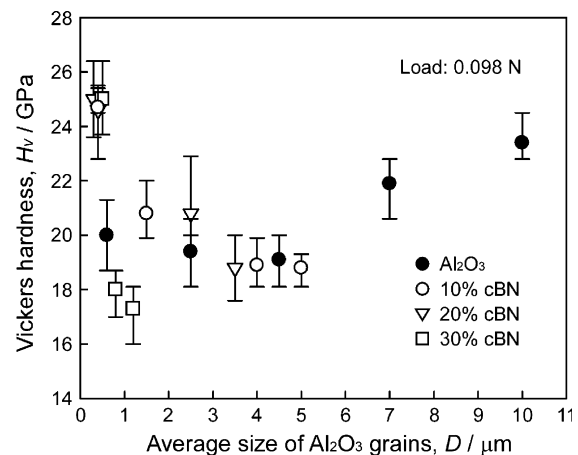


Fig. 2. Effect of average size of Al<sub>2</sub>O<sub>3</sub> grains in the monolithic Al<sub>2</sub>O<sub>3</sub> bodies and the Al<sub>2</sub>O<sub>3</sub>–BN composites on Vickers hardness of the Al<sub>2</sub>O<sub>3</sub> matrix at a load of 0.098 N.

increased with an increase in grain size ranging from 4.5 to 10  $\mu\text{m}$ . The Vickers hardness of ceramics such as  $\text{Al}_2\text{O}_3$  and  $\text{MgO}$  first decreased with increasing grain size, then increased toward that of single-crystals as the grain size increased to more than the indentation size [17]. The indentation size measured at a load of 0.098 N in the monolithic  $\text{Al}_2\text{O}_3$  bodies and the  $\text{Al}_2\text{O}_3$  matrix in the  $\text{Al}_2\text{O}_3$ –BN composites was around 3  $\mu\text{m}$ . Consequently, the calculated hardness value of the monolithic  $\text{Al}_2\text{O}_3$  bodies with the grain size of 4.5–10  $\mu\text{m}$  prepared at 1400–1600  $^\circ\text{C}$  might indicate the hardness of one crystal grain (i.e.,  $\text{Al}_2\text{O}_3$  single-crystal), resulting in the increase of the hardness with further increase of the grain size.

The hardness of the  $\text{Al}_2\text{O}_3$  matrix in the  $\text{Al}_2\text{O}_3$ –BN composites decreased with increasing size of the  $\text{Al}_2\text{O}_3$  grains. When sintering temperature increased, the size of  $\text{Al}_2\text{O}_3$  grains in the  $\text{Al}_2\text{O}_3$  bodies and the  $\text{Al}_2\text{O}_3$ –BN composites increased [10]. Hence, the reduction of the hardness of  $\text{Al}_2\text{O}_3$  matrix in the  $\text{Al}_2\text{O}_3$ –BN composites with increasing sintering temperature in Fig. 1 would be caused by the increase of the size of the  $\text{Al}_2\text{O}_3$  grains. The addition of cBN to  $\text{Al}_2\text{O}_3$  led to the decrease of the size of  $\text{Al}_2\text{O}_3$  grains in the  $\text{Al}_2\text{O}_3$ –BN composites [10]. Thus, the increase in the hardness of  $\text{Al}_2\text{O}_3$  matrix in the  $\text{Al}_2\text{O}_3$ –BN composites by the addition of cBN in Fig. 1 would be attributed to the decrease in the size of the  $\text{Al}_2\text{O}_3$  grains.

The Vickers hardness of ceramics might have been affected by many parameters, such as grain size, residual porosity, indentation load and bonding strength among grains [17]. Whereas all the specimens had high density of over 98%, the density of the  $\text{Al}_2\text{O}_3$ –BN composites was slightly lower than that of the monolithic  $\text{Al}_2\text{O}_3$  bodies. The decrease of the density would be attributed to the existence of residual pores at the interface between BN and  $\text{Al}_2\text{O}_3$  matrix due to the addition of low-sinterable cBN to  $\text{Al}_2\text{O}_3$ . Consequently, the  $\text{Al}_2\text{O}_3$  matrix in the  $\text{Al}_2\text{O}_3$ –BN composites might be fully dense, although the  $\text{Al}_2\text{O}_3$ –BN composites had slightly lower density compared with the monolithic  $\text{Al}_2\text{O}_3$  bodies.

### 3.3. Vickers indents in $\text{Al}_2\text{O}_3$ body and $\text{Al}_2\text{O}_3$ –BN composite

Fig. 3 shows SEM micrographs of the surfaces of a monolithic  $\text{Al}_2\text{O}_3$  body prepared at 1200  $^\circ\text{C}$  and a  $\text{Al}_2\text{O}_3$ –20 vol% cBN composite prepared at 1300  $^\circ\text{C}$  after Vickers indentation at loads of 0.98 and 9.8 N. The black phase is BN grains. The hardness value of the  $\text{Al}_2\text{O}_3$ –BN composites measured at the indentation load of 0.98 and 9.8 N was confirmed to include hardness of both  $\text{Al}_2\text{O}_3$  matrix and BN grains. The indentation size of the  $\text{Al}_2\text{O}_3$ –BN composite was smaller than that of the monolithic  $\text{Al}_2\text{O}_3$  body at 0.98 N, demonstrating that the hardness of the  $\text{Al}_2\text{O}_3$ –cBN composite was higher than that of the monolithic  $\text{Al}_2\text{O}_3$  body. Therefore, the improvement of the hardness of  $\text{Al}_2\text{O}_3$ –BN composites measured at indentation load of 0.98 N by the addition of cBN particles might be due to the existence of high-hardness cBN particles in the  $\text{Al}_2\text{O}_3$ –BN composites and the increase in hardness of  $\text{Al}_2\text{O}_3$  matrix, as shown in Figs. 1 and 2. In fact, in the  $\text{Al}_2\text{O}_3$ –BN composite originally containing 30 vol% cBN

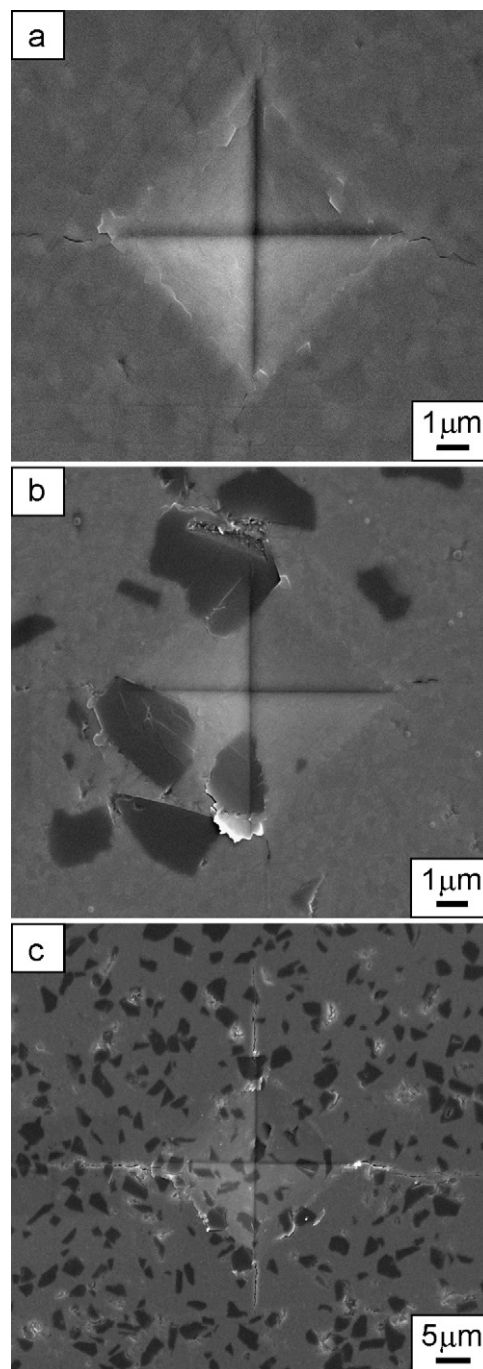


Fig. 3. SEM micrographs of indented surface of  $\text{Al}_2\text{O}_3$  body sintered at 1200  $^\circ\text{C}$  at a load of 0.98 N (a),  $\text{Al}_2\text{O}_3$ –BN composite originally containing 20 vol% cBN sintered at 1300  $^\circ\text{C}$  at load of 0.98 N (b) and that at load of 9.8 N (c).

prepared at 1400  $^\circ\text{C}$ , the Vickers hardness of the  $\text{Al}_2\text{O}_3$ –BN composite at 0.98 N reached maximum value of 26 GPa, although the cBN phase in the composite slightly transformed to hBN [10]. This might be caused by the small size of  $\text{Al}_2\text{O}_3$  grains of 0.5  $\mu\text{m}$  in the  $\text{Al}_2\text{O}_3$ –BN composite. Although some cracks can be seen at the  $\text{Al}_2\text{O}_3$ /cBN interface in the  $\text{Al}_2\text{O}_3$ –BN composite, it was possible for bonding between the  $\text{Al}_2\text{O}_3$  matrix and the cBN grains to remain strong even under the high indentation load of 9.8 N.

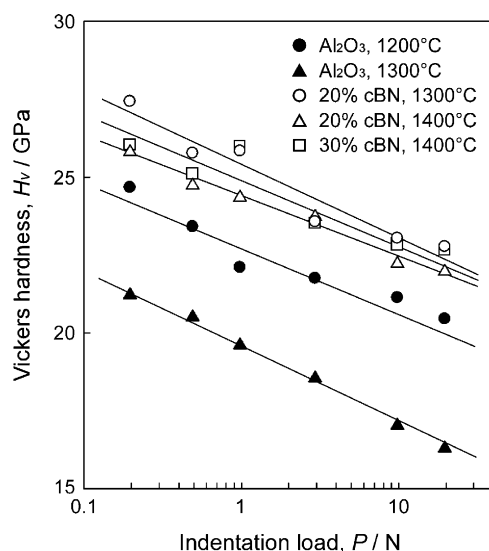


Fig. 4. Vickers hardness of  $\text{Al}_2\text{O}_3$ –BN composites originally containing 20–30 vol% cBN and  $\text{Al}_2\text{O}_3$  bodies sintered at 1200–1400 °C as a function of applied indentation load.

### 3.4. Load dependence of hardness of $\text{Al}_2\text{O}_3$ bodies and $\text{Al}_2\text{O}_3$ –BN composites

Fig. 4 shows the load dependence of Vickers hardness of monolithic  $\text{Al}_2\text{O}_3$  bodies and  $\text{Al}_2\text{O}_3$ –BN composites originally containing 20–30 vol% cBN prepared at different temperatures. The hardness of both the monolithic  $\text{Al}_2\text{O}_3$  bodies and the  $\text{Al}_2\text{O}_3$ –BN composites increased with decreasing indentation load. The hardness generally increases with decreasing indentation load, as has been reported in  $\text{Si}_3\text{N}_4$ , SiC, cBN and Ce– $\text{ZrO}_2$  [18–21]. This is often termed the indentation size effect. Krell [19] has reported that a fully dense  $\text{Al}_2\text{O}_3$  body with a grain size of 0.45  $\mu\text{m}$  exhibited an increase in hardness with decreasing load and that the hardness reached its highest value of 22 GPa at 6 N. At each indentation load of 0.196–19.6 N, the hardness of the monolithic  $\text{Al}_2\text{O}_3$  body prepared at 1200 °C was 2–4 GPa higher than that prepared at 1300 °C. The grain size of  $\text{Al}_2\text{O}_3$  bodies prepared at 1200 °C and 1300 °C was less than 1  $\mu\text{m}$  and about 3  $\mu\text{m}$ , respectively [10]. On the contrary, Krell and Blank [16] have reported that the hardness of the fully dense  $\text{Al}_2\text{O}_3$  body at load of 100 N decreased with increasing grain size. The hardness of  $\text{Al}_2\text{O}_3$ –BN composites originally containing 20–30 vol% cBN prepared at 1300–1400 °C was higher than that of monolithic  $\text{Al}_2\text{O}_3$  bodies at each indentation load.

Table 1 summarizes the Meyer exponents determined by the results shown in Fig. 4 in comparison with literature data [22]. The Meyer exponents of the monolithic  $\text{Al}_2\text{O}_3$  bodies and  $\text{Al}_2\text{O}_3$ –cBN composites were 1.90–1.94, close to those of common oxide ceramics such as  $\text{ZrO}_2$  and mullite, but greater than those of SiC and  $\text{Si}_3\text{N}_4$ . This implies that SiC and  $\text{Si}_3\text{N}_4$  show more significant load dependence of hardness. Although the physical meaning of the Meyer exponent is not fully understood, it may be related to several deformation characteristics such as partial elastic deformation and viscous

Table 1

Values of the Meyer exponent of  $\text{Al}_2\text{O}_3$ –BN composites originally containing 20–30 vol% cBN and of  $\text{Al}_2\text{O}_3$  bodies sintered at 1200–1400 °C.

Specimens	Sintering temperature, $T$ (°C)	Meyer exponent, $n$
$\text{Al}_2\text{O}_3$	1200	1.92
$\text{Al}_2\text{O}_3$	1300	1.90
$\text{Al}_2\text{O}_3$ –20 vol% cBN	1300	1.93
$\text{Al}_2\text{O}_3$ –20 vol% cBN	1400	1.93
$\text{Al}_2\text{O}_3$ –30 vol% cBN	1400	1.94
$\text{Al}_2\text{O}_3^a$	–	1.89
$\text{ZrO}_2^a$	–	1.91
Mullite <sup>a</sup>	–	1.98
SiC <sup>a</sup>	–	1.79
$\text{Si}_3\text{N}_4^a$	–	1.84

<sup>a</sup> Data of Gong et al. [22].

flow of materials. It can be assumed that a different Meyer exponent means a different deformation mechanism. The deformation mechanism during the Vickers hardness measurement may be independent of cBN content in the  $\text{Al}_2\text{O}_3$ –BN composites, whereas it can be slightly different from that of more covalent bonding ceramics such as SiC and  $\text{Si}_3\text{N}_4$ .

## 4. Conclusions

The Vickers hardness of dense  $\text{Al}_2\text{O}_3$ –cBN composites prepared by SPS at a moderate pressure of 100 MPa was characterized at indentation loads from 0.098 to 19.6 N. The hardness of BN grains in the  $\text{Al}_2\text{O}_3$ –BN composite prepared at 1300 °C without the phase transformation of cBN to hBN was 59 GPa at load of 0.098 N. The hardness of the BN grains decreased to 57 GPa at 1400 °C due to a slight phase transformation from cBN to hBN. The hardness of the  $\text{Al}_2\text{O}_3$  matrix in the  $\text{Al}_2\text{O}_3$ –BN composites increased with decreasing sintering temperature. The hardness of the  $\text{Al}_2\text{O}_3$  matrix in  $\text{Al}_2\text{O}_3$ –BN composites originally containing 10–30 vol% cBN prepared at 1300–1400 °C increased by about 5 GPa compared with that of monolithic  $\text{Al}_2\text{O}_3$  bodies prepared at the same temperature. The improvement of the hardness of the  $\text{Al}_2\text{O}_3$  matrix in the  $\text{Al}_2\text{O}_3$ –BN composites may be attributed to the decrease in the size of  $\text{Al}_2\text{O}_3$  grains due to the decrease in sintering temperature and due to the addition of cBN particles. The hardness of both the monolithic  $\text{Al}_2\text{O}_3$  bodies and the  $\text{Al}_2\text{O}_3$ –BN composites increased with a decrease in indentation load. The Meyer exponents were 1.90–1.94, independent of cBN content.

## Acknowledgements

This work was supported by a Grant-in-Aid for Young Scientists (Start-up) (No. 18860009), the Asian CORE Program and the Global COE Program “Materials Integration, Tohoku University,” MEXT, Japan and the Rare Metal Substitution Materials Development Project of the New Energy and Industrial Technology Development Organization. We also appreciate the financial support of Mitsubishi Materials Corporation.



## References

- [1] P. Klimczyk, E. Benko, K. Lawniczak-Jablonska, E. Piskorska, M. Heinonen, A. Ormaniec, W. Gorczynska-Zawislan, V.S. Urbanovich, Cubic boron nitride–Ti/TiN composites: hardness and phase equilibrium as function of temperature, *Journal of Alloys and Compounds* 382 (1–2) (2004) 195–205.
- [2] X.Z. Rong, T. Yano, TEM investigation of high-pressure reaction-sintered cBN–Al composites, *Journal of Materials Science* 39 (14) (2004) 4705–4710.
- [3] X.Z. Rong, T. Tsurumi, O. Fukunaga, T. Yano, High-pressure sintering of cBN–TiN–Al composite for cutting tool application, *Diamond and Related Materials* 11 (2) (2002) 280–286.
- [4] X.Z. Rong, O. Fukunaga, Sintering of cubic boron nitride with added aluminum at high pressure and high temperatures, *Transactions of the Materials Research Society of Japan* 14B (1994) 1455–1458.
- [5] V.L. Solozhenko, V.Z. Turkevich, W.B. Holzapfel, Refined phase diagram of boron nitride, *Journal of Physical Chemistry B* 103 (15) (1999) 2903–2905.
- [6] F.R. Corrigan, F.P. Bundy, Direct transitions among the allotropic forms of boron nitride at high pressures and temperatures, *Journal of Chemical Physics* 63 (9) (1975) 3812–3820.
- [7] F.P. Bundy, R.H. Wentorf Jr., Direct transformation of hexagonal boron nitride to denser forms, *Journal of Chemical Physics* 38 (5) (1963) 1144–1149.
- [8] H. Moriguchi, K. Tsuduki, A. Ikegaya, When diamonds and CBN are a driller's best friends, *Metal Powder Report* 59 (4) (2004) 26–30.
- [9] V. Martínez, J. Echeberria, Hot isostatic pressing of cubic boron nitride–tungsten carbide/cobalt (cBN–WC/Co) composites: effect of cBN particle size and some processing parameters on their microstructure and properties, *Journal of the American Ceramic Society* 90 (2) (2007) 415–424.
- [10] M. Hotta, T. Goto, Densification and microstructure of  $\text{Al}_2\text{O}_3$ –cBN composites prepared by spark plasma sintering, *Journal of the Ceramic Society of Japan* 116 (6) (2008) 744–748.
- [11] M. Hotta, T. Goto, Densification and phase transformation of  $\beta$ -SiAlON–cubic boron nitride composites prepared by spark plasma sintering, *Journal of the American Ceramic Society* 92 (8) (2009) 1684–1690.
- [12] M. Hotta, T. Goto, Spark plasma sintering of TiN–cubic BN composites, *Journal of the Ceramic Society of Japan* 118 (2) (2010) 137–140.
- [13] M. Hotta, T. Goto, Densification, phase transformation and hardness of mullite–cubic BN composites prepared by spark plasma sintering, *Journal of the Ceramic Society of Japan* 118 (2) (2010) 157–160.
- [14] N.C. Dunegan, in: W.W. Krieger, H. Palmour, III (Eds.), *Mechanical Properties of Engineering Ceramics*, Interscience Publisher, New York, 1960, p. 521.
- [15] S.D. Skrovaneck, R.C. Bradt, Microhardness of a fine-grain-size  $\text{Al}_2\text{O}_3$ , *Journal of the American Ceramic Society* 62 (3–4) (1979) 215–216.
- [16] A. Krell, P. Blank, Grain size dependence of hardness in dense submicrometer alumina, *Journal of the American Ceramic Society* 78 (4) (1995) 1118–1120.
- [17] R.W. Rice, C.C. Wu, F. Borchelt, Hardness–grain size relations in ceramics, *Journal of the American Ceramic Society* 77 (10) (1994) 2539–2553.
- [18] T. Taniguchi, M. Akaishi, S. Yamaoka, Mechanical properties of polycrystalline translucent cubic boron nitride as characterized by Vickers indentation method, *Journal of the American Ceramic Society* 79 (2) (1996) 547–549.
- [19] A. Krell, Load dependence of hardness in sintered submicrometer  $\text{Al}_2\text{O}_3$  and  $\text{ZrO}_2$ , *Journal of the American Ceramic Society* 78 (5) (1995) 1417–1419.
- [20] R. Berriche, R.T. Holt, Effect of load on the hardness of hot isostatically pressed silicon nitride, *Journal of the American Ceramic Society* 76 (6) (1993) 1602–1604.
- [21] M.-O. Guillou, J.L. Henshall, R.M. Hooper, G.M. Carter, Indentation fracture testing and analysis, and its application to zirconia, silicon carbide and silicon nitride ceramics, *Journal of Hard Materials* 3 (3–4) (1992) 421–434.
- [22] J. Gong, J. Wu, Z. Guan, Examination of the indentation size effect in low-load Vickers hardness testing of ceramics, *Journal of the European Ceramic Society* 19 (15) (1999) 2625–2631.